SUPPLEMENTARY INFORMATION

Supplementary Material and Methods

Plasmids

Plasmids used in the study are described in **Table S1**. Site-directed mutagenesis was performed by PCR to introduce desired mutations in the Nix constructs. The correctness of the DNA sequence was verified by sequencing.

Antibodies and reagents

The following antibodies were used in the study: mouse monoclonal anti-Nix (Sigma, 1:4000); mouse monoclonal anti-Flag M2 (Sigma, 1:10,000); mouse monoclonal anti-GST (Santa Cruz Biotechnology; 1:3000); rabbit polyclonal anti-GFP (Clontech, 1:1000); anti-LC3 (a kind gift form Z. Elazar). Secondary HRP conjugated antibodies, goat anti-mouse and goat anti-rabbit IgGs were used for immunoblotting. Donkey anti-mouse Cy3-conjugated secondary antibody (Jackson Immuno Research) was used for immunofluorescence studies. Mitotracker Deep Red 633nm (MTDR) (Invitrogen) was used as a marker of mitochondria in confocal microscopy. Carbonylcyanide 3-Chlorophenylhydrazone (CCCP) (Sigma) was applied to cells at a final concentration of 10 μM and Rotenone (Sigma) - at a final concentration of 5 μM for 3 hrs.

Yeast re-transformation assay

Y190 yeast clones expressing UBLs were transformed with plasmids encoding interaction partners **(Table S1)**. Colonies were plated on selective media and β-galactosidase assay was performed using X-gal as a substrate.

Preparation of GST-fusion proteins

GST fusions of various proteins **(Table S1)** were expressed in BL21 *E. coli*. Fusion protein expression was induced by adding 0.5 mM IPTG for 4 hrs. Bacteria were lysed in 20 mM Tris-HCl, pH7.5, 10 mM EDTA, pH8.0, 5 mM EGTA, 150 mM NaCl supplemented with 2 mg/ml lysozyme. GST fusion proteins were subsequently bound to pre-washed Glutathione-Sepharose 4B beads (GE Healthcare). After several washes, fusion protein-bound beads were used directly in binding assays.

GST pull-down assay

HEK293 or COS7 cells were transfected with expression constructs encoding the protein of interest using Lipofectamine2000 (Invitrogen). 24-36 hrs post-transfection cells were lysed in 50 mM HEPES, pH7.5, 150 mM NaCl, 1 mM EDTA, 1 mM EGTA, 10% glycerol, 1% Triton X-100, 25 mM NaF, 50 mM ZnCl2 and lysates were incubated overnight with immobilized GST-fusion proteins. Following 5 washes, beads with co-precipitated proteins were resuspended in 2x SDS-PAGE loading buffer, boiled and loaded onto 10% or 12% SDS-PAGE gels for analysis.

Immunoprecipitation

For the immunoprecipitation experiments HeLa cells were lysed in ice-cold lysis buffer (50 mM Tris-HCl pH 7.5, 150 mM NaCl, 1 mM $MgCl_2$, 0,1% SDS) supplemented with protease inhibitor coctail (Roche). The lysates were pre-cleared by 15 minutes centrifugation at 2.500 rpm in a microcentrifuge at 4°C. To the cleared lysate monoclonal

anti-Nix was added and rotated overnight at 4°C. Immunocomplexes collected by adding 20 µl of protein A conjugated agarose bead solution (Santa Cruz Biotechnology) for one hour and washed in lysis buffer for five times. Finally, beads were resuspended in 20 µl 2x SDS-PAGE gel load buffer, boiled and detected by immunoblot analysis using chemoluminescence based detection.

Nuclear Magnetic Resonance (NMR) spectroscopy and Isothermal Titration Calorimetry (ITC)

Unlabeled and labeled (^{15}N or ^{13}C-^{15}N) human Atg8 protein family members were expressed as GST-fusion proteins in DH5α *E. coli* in LB or M9 media. Proteins were isolated by glutathione affinity chromatography, cleaved from the GST moiety by thrombin treatment and purified by size-exclusion chromatography. Proteins were equilibrated in 25 mM NaPi, 150 mM NaCl buffer, pH7.5. The solid-phase synthesized, lyophilized peptides p62-LIR, Nix-W139/143 and Nix-W35 were solubilized in 25 mM NaPi, 150 mM NaCl buffer, pH7.5 to prepare stock solutions. Titration of ^{15}N-labeled proteins (~100µM) with p62-LIR1, Nix-W35 and Nix-W139/143 was performed at 25°C by gradually adding stock solutions of unlabeled peptides. To monitor binding-induced changes in protein resonances, ^{15}N-^{1}H HSQC-TROSY spectra were recorded on Bruker Avance spectrometers operating at proton frequencies 600 and 700 MHz. Three residues were selected to represent areas in proximity to HP1 (I34), HP2 (R70) and distant to both (G/Q85). The exact positions of these residues are shown in **Fig. S1B**. For these residues, individual K_D were calculated according to (Eldridge et al., 2002). For ITC, proteins were equilibrated in 25 mM NaPi, 150 mM NaCl buffer, pH7.5. For LC3/p62-LIR

experiments, 400 µM p62-LIR was titrated into 15 µM LC3 in 26 steps (10 µL per injection). For Nix peptides, 1.6 mM Nix-W35 was titrated into 80 µM LC3, and 2 mM Nix-W139/143 was titrated into 100 µM LC3 in 16 steps (15 µL per injection).

Laser Scanning Microscopy

Approximately 2 x 10^5 cells were seeded, grown on coverslips and transfected with either Wt or W35A Nix-Flag constructs using Fugene HD according to manufacturers' instructions. 24hrs post transfection, cells were pulsed with 200 nM Mitotracker Deep Red 633nm (Invitrogen) for 45 min. Cells were then washed twice with PBS and treated accordingly. Post-treatment cells were immediately fixed in 2% paraformaldehyde. Subsequently, cells were permeabilized with a 0.2% Triton X-100 solution in PBS at room temperature for 20 min. All cells were blocked in PBS containing 5% BSA at 4 °C overnight. Primary and secondary antibodies were diluted in the blocking solution, and washes were performed in 0.1% Tween 20 in PBS. Coverslips were mounted on 20 µl of aqueous mounting medium (Biomeda) placed on a glass holder. Image analysis and plot profiles were generated using the ImageJ software (http://rsbweb.nih.gov/ij/). In more detail, the co-localization highlighter was used (part of the WCIF ImageJ) to highlight the points of Nix and GFP-GABARAP-L1 co-localization (Fig.3A&B, white dots). Thresholds were determined using the mean intensity of each channel and calculated as 3x standard deviation. These data were factored into the co-localization program.

Retroviral-mediated gene transfer of Nix into Nix$^{-/-}$ mice

Wt and mutant Nix cDNAs were subcloned into the retroviral vector MSCV-Ires-GFP. To make viral producer cells, 1 x 10^6 293T cells were plated in a 10 cm dish, and transfected with 10 μg of plasmid DNA (4 μg viral DNA, 4 μg pEQ-Pam3 (-Env), and 2 μg pSRαG, or equivalent VSV-G envelope) (Persons et al., 2003) and 30 μl Fugene 6. Next, 1 x 10^5 GPE86 (+) cells were plated in a 10 cm dish. Every 12 hours viral supernatant from the transfected 293T cells was harvested, filtered, and applied to the GPE86 (+) cells, with 6 mg/ml polybrene (Sigma, St. Louis, MO), for a total of 6 applications. After the sixth application, the GPE86 (+) cells were harvested, sorted for GFP expression (highest 50% of expressing cells), and re-plated. Donor *Nix*$^{-/-}$ mice were prepared by a single intraperitoneal injection of 150 mg/kg 5-FU. Four days after administration of 5-FU, the virus producer cells were irradiated (3,000 rad), and 4 x 10^6 cells were plated in a 10 cm dish that had been coated with 1% gelatin. The following day, bone marrow was harvested from the femurs and tibias of the donor *Nix*$^{-/-}$ mice. After lysis of erythrocytes (BD Biosciences, San Jose, CA), bone marrow cells were washed once with PBS, and resuspended in DMEM with 15% FBS. Next, they were plated at a density of 1 x 10^6 cells/ml in 10 cm suspension dishes, and prestimulated for 36 hours with growth factors (50 ng/ml murine SCF (Peprotech Inc., Rocky Hill, NJ), 20 ng/ml murine IL-3 (Peprotech Inc., Rocky Hill, NJ), and 50 ng/ml IL-6 (BioVision Research Products, Mountain View, CA)). Following prestimulation, 5 x 10^5 bone marrow cells in 5 ml of fresh medium were added to each dish of producer cells, after removal of an equal volume of medium. Growth factors (the same as during prestimulation) and 6 μg/ml polybrene were added, and the cells were co-cultured for 36

hours. After co-culture, the transduced bone marrow cells were harvested and the cells from each dish used to transplant 3 lethally-irradiated (1000 rad) wild-type recipient mice.

Analysis of mitochondrial clearance

Reticulocytosis was induced by phenylhydrazine treatment, and reticulocyte-enriched blood was cultured and stained with MitoTracker Red, as previously described (Zhang et al., 2009a). Mitochondrial clearance was assessed in the GFP-positive fraction, which corresponds to virally transduced cells, with a BD LSR II flow cytometry analyzer, after excluding a minor autofluorescent cell population that arises from the phenylhydrazine treatment.

Supplementary references

Eldridge, A.M., Kang, H.S., Johnson, E., Gunsalus, R. and Dahlquist, F.W. (2002) Effect of phosphorylation on the interdomain interaction of the response regulator, NarL. *Biochemistry*, **41**, 15173-15180.

Ichimura, Y., Kumanomidou, T., Sou, Y.S., Mizushima, T., Ezaki, J., Ueno, T., Kominami, E., Yamane, T., Tanaka, K. and Komatsu, M. (2008) Structural basis for sorting mechanism of p62 in selective autophagy. *J Biol Chem*, **283**, 22847-22857.

Supplementary figure legends

Figure S1. *Isothermal Titration Calorimetry (ITC) and Nuclear Magnetic Resonance (NMR) analyses of the interaction of Nix-LIR peptides with LC3 proteins.* **A.** LIR peptides used in the study. **B**. The top diagrams display the raw measurement data and the bottom diagrams show the integrated heat per titration step. All titration experiments with indicated LIR peptide:LC3 protein pairs were performed with 150 mM NaCl at 25° C. **C**. K_D values, as calculated from CSP data for selected LC3A and LC3B resonances (I34, R70 and G/Q85 **Fig. S1D**, left plot) upon titration with Nix–LIR peptides. **D.** Left plot: structure of the LC3B:p62 complex (PDB ID 2ZJD, (Ichimura et al., 2008)). The residues selected for K_D calculations are shown in cyan. Right plot: CSP mapping of p62-LIR on LC3B structure (all residues whose resonances show "two-state" transition are marked red). **E.** The SCP for Nix-W35 (bottom, left) and Nix-W139/143 (bottom, right) were categorized as followed: below 0.03/0.04 ppm – gray, 0.03/0.04 ppm – 0.08/0.10 ppm – yellow, bigger than 0.08/0.10 ppm – red (for Nix-W35 and Nix-W139/143, respectively).

Figure S2. *Nix recruits EGFP-GABARAP-L1 to stressed mitochondria in HeLa cells.* **A., B.** HeLa cells co-transfected with EGFP-GABARAP-L1 and Wt-Nix (**A.**) or Nix W35A (**B.**) were incubated with and without mitochondrial poisons (rotenone and CCCP) for 3 hrs. Cells were then fixed and analyzed for the co-localization between mitochondria (MTR), EGFP-GABARAP-L1 and Nix (stained with anti-Nix-Cy3 antibody). **C.** Quantification was achieved by counting the number of complete co-localizations (EGFP/Cy3/Mito) per cell for approximately 100 cells per condition. Results are

expressed as a fold change in Wt-Nix, control treated cells. Error bars reflect Standard Error of Mean (SEM). **.** Levels of endogenous and overexpressed Wt-Nix or Nix-W35A.

Figure S3. *EGFP-GABARAP-L1 co-localization with MitoTracker in* $Nix^{+/+}$ *and* $Nix^{-/-}$ *cells.* **A.** $Nix^{+/+}$ *or* **B**. $Nix^{-/-}$ cells co-transfected with EGFP-GABARAP-L1 and Wt-Nix were incubated with and without mitochondrial poisons (rotenone and CCCP) for 3 hrs. Cells were then fixed and analyzed for the co-localization between mitochondria (MTR) and EGFP-GABARAP-L1. **C.** Quantification was achieved by counting the number of complete co-localizations EGFP/MTR per cell for approximately 30 cells per condition. Results are expressed as a fold change.

Figure S4. *Role of Nix and ubiquitin in mitophagy*. Mitochondrion-localized Nix interacts via its N-terminal LIR with LC3/GABARAP-conjugated to the autophagosome thereby mediating tethering of the nascent autophagosome to the target mitochondrion. Concomitant ubiquitination of a mitochondrion-localized substrate protein may, via Ub-binding autophagy receptors (p62 and NBR1), further increase tethering of mitochondrial and autophagosomal membranes.

Table S1. Plasmids used in the study.

Vector	Description	Source
pACT2	Y2H prey vector	Clontech
pACT2-ATG4A(245-336)	Y2H prey vector encoding C-terminal part of human ATG4A	this study
pACT2-ATG4B(58-393)	Y2H prey vector encoding C-terminal part of	this study

	human ATG4B	
pACT2-NBR1(691-966)	Y2H prey vector encoding C-terminal part of human NBR1	(Kirkin et al., 2009)
pACT2-p62(311-444)	Y2H prey vector encoding C-terminal part of human p62	(Kirkin et al., 2009)
pACT2-Nix	Y2H prey vector encoding full-length human NIX	this study
pcDNA3.1(-)/Flag-Nix	Flag-tagged mouse Nix	(Yussman et al., 2002)
pcDNA3.1(-)/Flag-Nix(W35A)	Flag-tagged mouse Nix, W35 mutated to Ala	this study
pcDNA3.1(-)/Flag-Nix(W139A)	Flag-tagged mouse Nix, W139 mutated to Ala	this study
pcDNA3.1(-)/Flag-Nix(W143A)	Flag-tagged mouse Nix, W143 mutated to Ala	this study
pcDNA3.1(-)/Flag-Nix(W35A&L38A)	Flag-tagged mouse Nix, W35 and L38 mutated to A	this study
pcDNA3.1(-)/Flag-Nix(Δ35-38)	Flag-tagged mouse Nix, ΔLIR (ΔWVEL)	this study
pcDNA3.1(-)/Flag-Nix(Δ39)	Flag-tagged mouse Nix, ΔN-term	this study
pGEX-4T-1/Nix(ΔTM)	GST-tagged mouse Nix, ΔC-term (1-182)	this study
pGEX-4T-1/scAtg8	GST-tagged Atg8 (from *S. cerevisiae*)	(Kirkin et al., 2009)
pGEX-4T-1/hGABARAP	GST-tagged human GABARAP	(Kirkin et al., 2009)
pGEX-4T-1/hGABARAP-L1	GST- tagged human GABARAP-L1	(Kirkin et al., 2009)
pGEX-4T-1/hGABARAP-L2	GST-tagged human GABARAP-L2	(Kirkin et al., 2009)
pGEX-4T-1/hLC3-A	GST-tagged human LC3-A	(Kirkin et al., 2009)
pGEX-4T-1/hLC3-B	GST-tagged human LC3-B	(Kirkin et al., 2009)
pGEX-4T-1/SUMO1	GST-tagged SUMO1	
pGEX-4T-1/Ub	GST-tagged Ub	
pGEX-4T-1	GST fusion expression vector	GE Healthcare
pYTH9-SUMO1	Y2H bait vector encoding human SUMO-1	(Hecker et al., 2006)
pYTH9-ATG8	Y2H bait vector encoding *S. cerevisiae* ATG8	(Kirkin et al., 2009)
pYTH9-LC3B	Y2H bait vector encoding human LC3B	(Kirkin et al., 2009)
pYTH9-ATG12	Y2H bait vector encoding human ATG12	(Kirkin et al., 2009)

Suplementary Figure S1

A.

Synthetic peptides used:

p62-LIR:	22 aa	RPEEQMESDNCSGGDDDWTHLS
Nix-W35:	15 aa	GLNSSWVELPMNSSN
Nix-W139/W143	16 aa	SADWVSDWSSRPENIP

B.

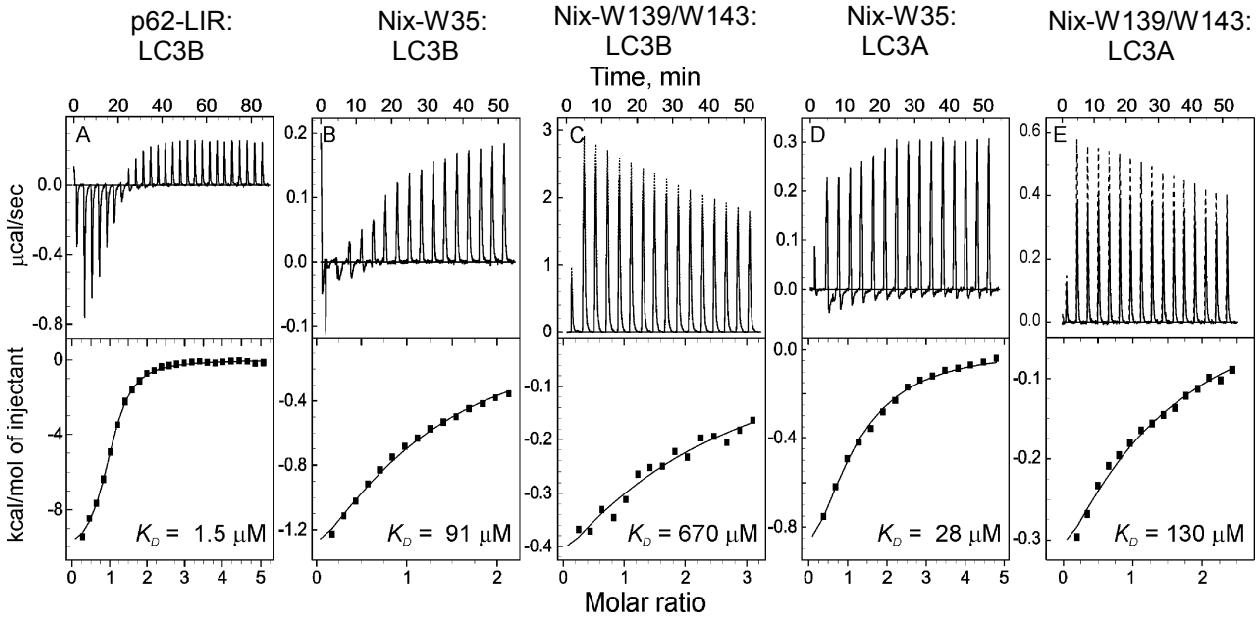

C.

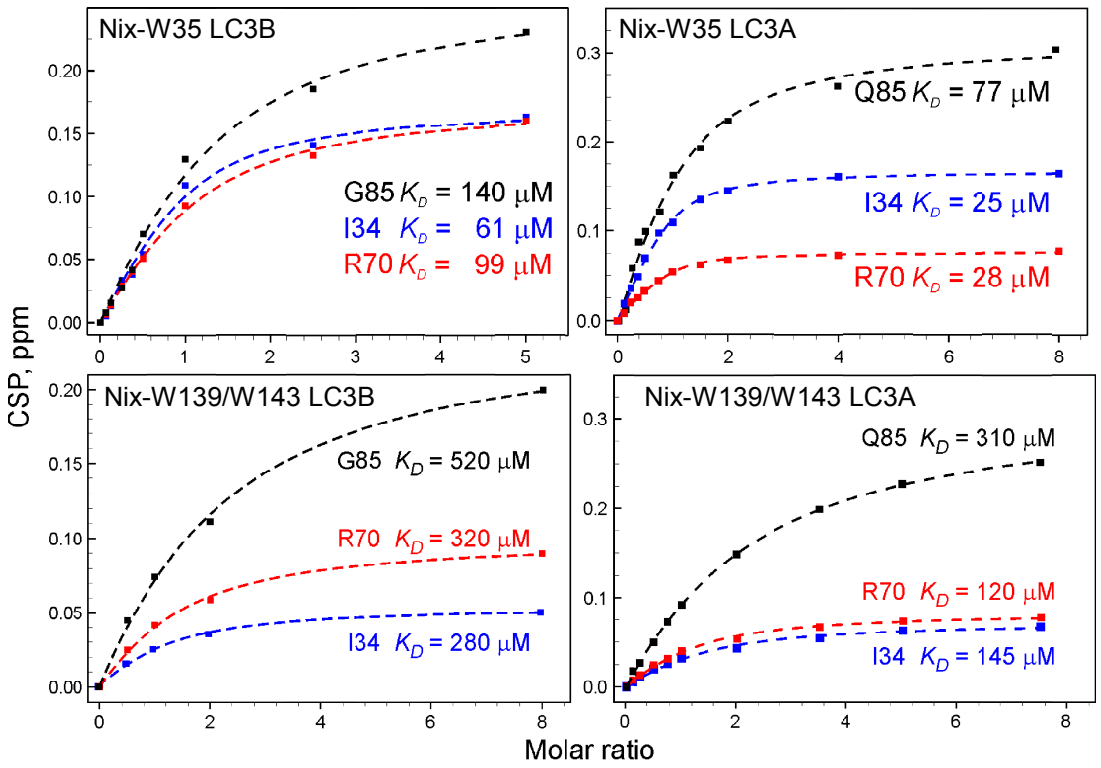

Suplementary Figure S1

D.

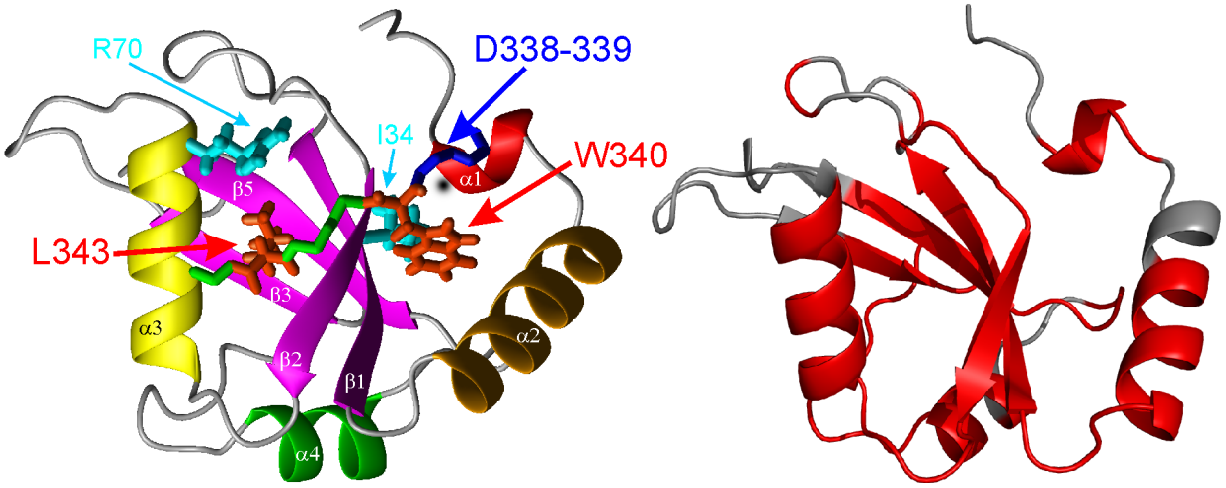

E.

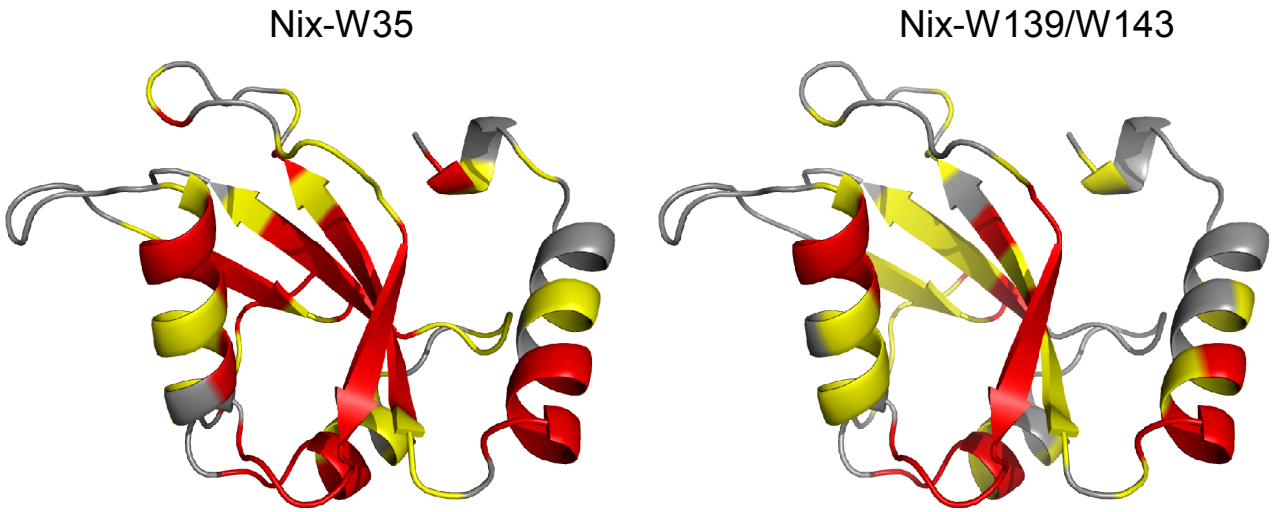

Supplemental Figure 2

(A) HeLa Nix-Flag Wt/EGFP-GABARAP-L1

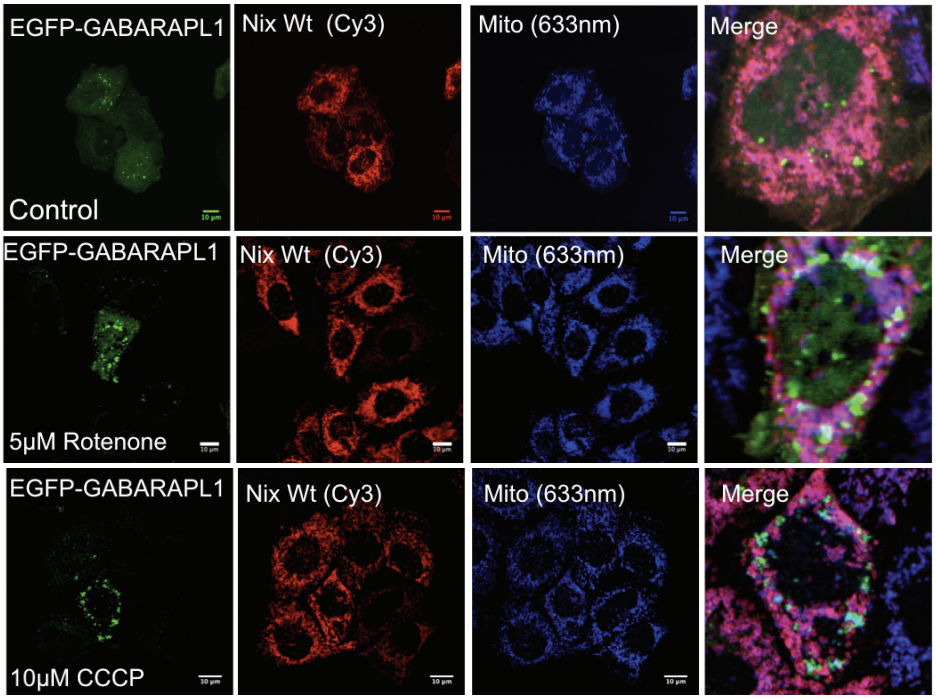

(B) HeLa Nix-Flag W35A/EGFP-GABARAP-L1

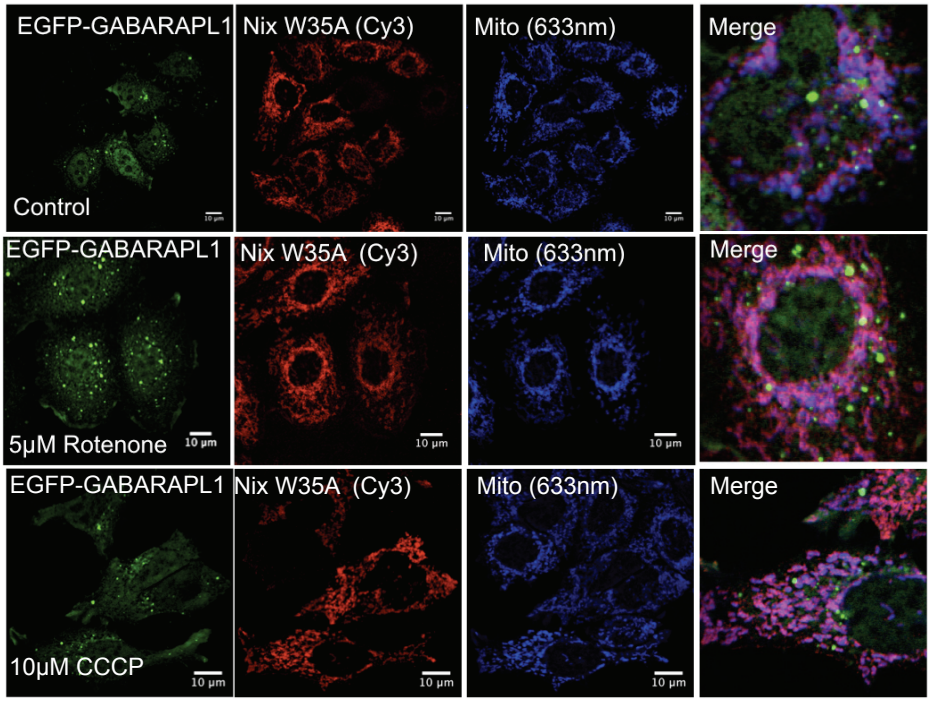

Figure S2 cont.

(C) Nix Co-localization with EGFP-GABARAP-L1 & Mitotracker in HeLa cells

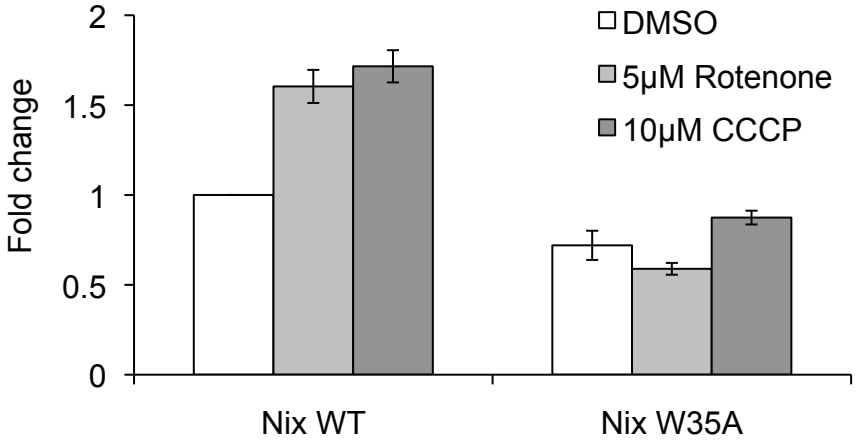

(D) Total Nix protein levels in transfected HeLa cells

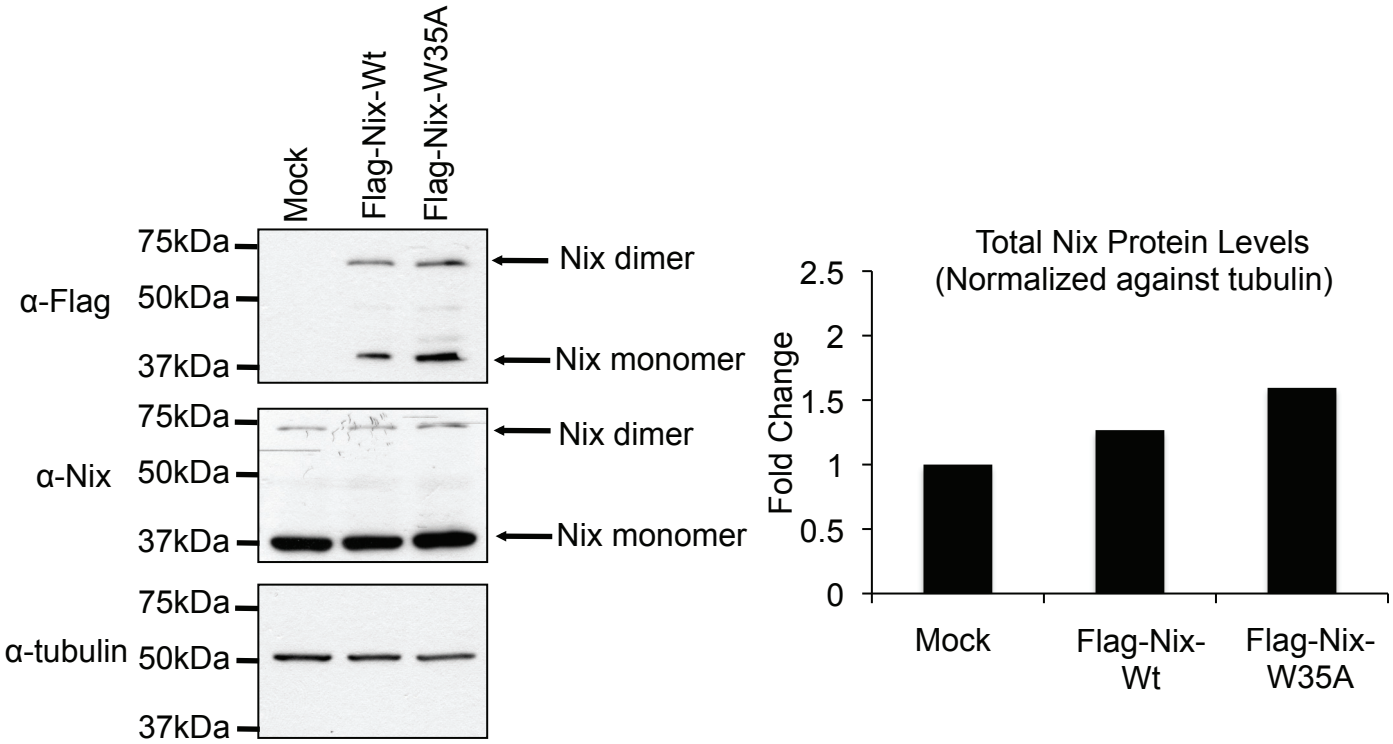

Supplemental Figure 3

A. *Nix*$^{+/+}$ MEFs EGFP-GABARAP-L1 *vs* Mitotracker (633nm)

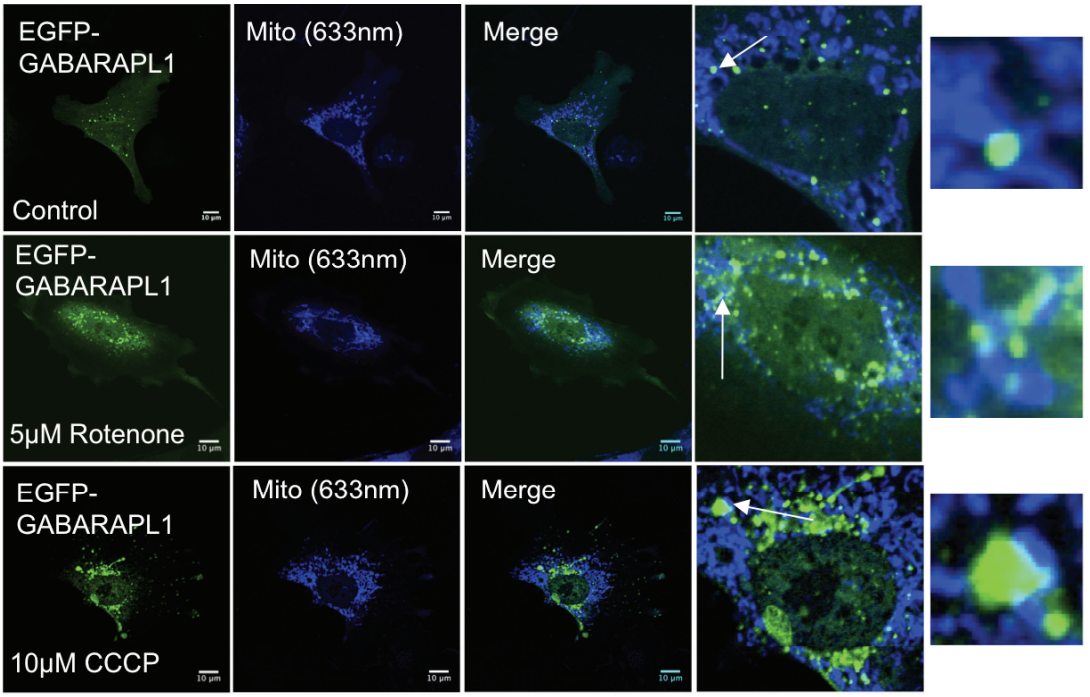

B. *Nix*$^{-/-}$ MEFs EGFP-GABARAP-L1 *vs* Mitotracker (633nm)

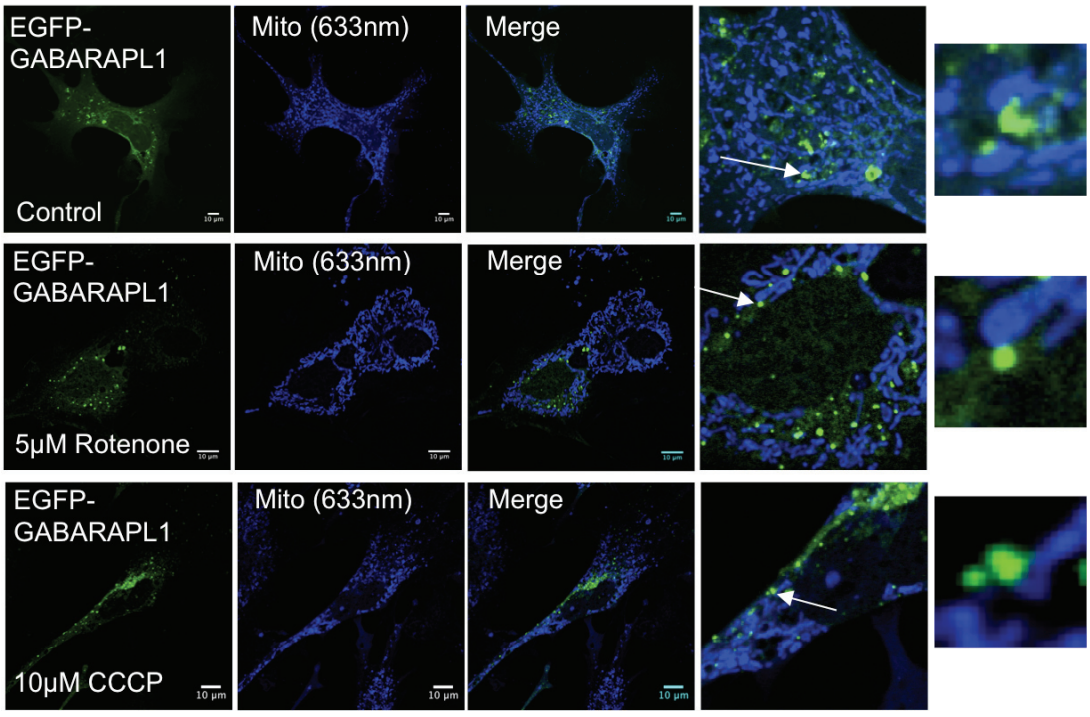

Supplemental Figure 3. cont.

c.

EGFP-GABARAP-L1 Co-localization vs. Mitotracker in *Nix*$^{-/-}$ and *Nix*$^{+/+}$ MEFs

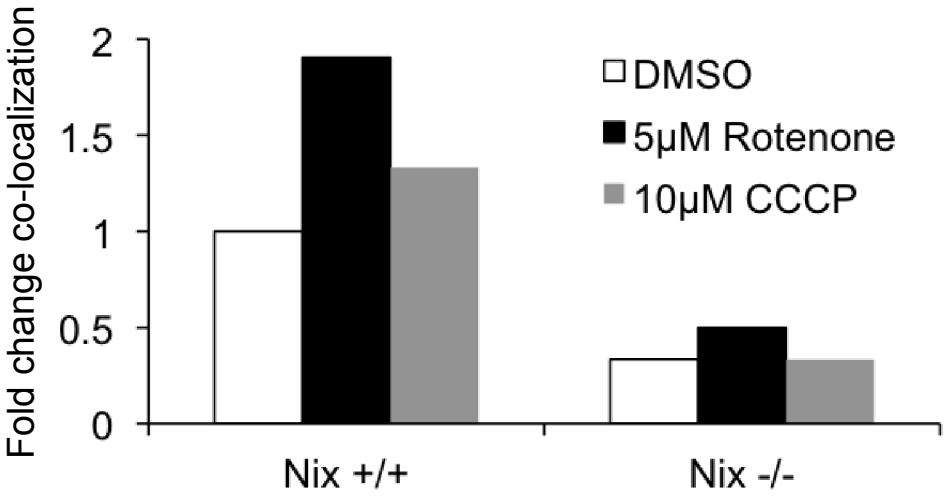

Supplementary Figure S4